IMPACT OF SURFACE TEXTURE ON NATURAL CONVECTION BOUNDARY-LAYER OF NANOFLUID

by

Ahmer MEHMOOD and Muhammad SALEEM IQBAL *

Department of Mathematics and Statistics, FBAS, International Islamic University, Islamabad, Pakistan

Original scientific paper
https://doi.org/10.2298/TSCI151008122M

Heat transfer characteristics are investigated in natural convection flow of water-based nanofluid near a vertical rough wall. The analysis considers five different nanoparticles: silver, copper, alumina, magnetite, and silica. The concentration has been limited between 0-20% for all types of nanoparticle. The governing equations are modeled using the Boussinesq approximation and Tiwari and Das models are utilized to represent the nanofluid. The analysis examines the effects of nanoparticle volume fraction, type of nanofluid, and the wavy surface geometry parameter on the skin friction and Nusselt number. It is observed that for a given nanofluid the skin friction and Nusselt number can be maximized via an appropriate tuning of the wavy surface geometry parameter along with the selection of suitable nanoparticle. Particular to this study cooper is observed to be more productive towards the flow and heat transfer enhancement. In total the metallic oxides are found to be less beneficial as compared to the pure metals.

Key words: *nanofluid, natural convection, heat transfer, wavy surface*

Introduction

Natural convection flow occurs due to the buoyancy force caused by temperature difference between the solid surface and the ambient fluid. The free convection flows happen frequently in natural and in engineering phenomenon. For example, the buoyant flow occurs from heat rejection to the atmosphere, heating and cooling of rooms and buildings, flow driven by temperature and salinity differences in oceans, flows generated by fire and in weather systems convection cells formed from air raising above heated land or water, *etc.*, in natural processes. The cooling of molten metals and fluid flows around shrouded heat dissipation fins and solar ponds are also the examples of natural convection applications in engineering processes. Furthermore, the natural convection also takes place in various phenomenons such as fire engineering, combustion modeling, nuclear reactor cooling, heat exchangers, petroleum reservoirs, *etc.* The study of heat transfer in natural convection flow belongs to an important class of boundary-layer flows. The quantity of heat transferred (to or from the fluid) is highly dependent upon the flow character and surface texture within the boundary-layer. In radiator, heat exchangers and heat transfer enhancement devices their surface is made intentionally rough and irregular in order to enhance the heat transfer rates. The waviness and increased surface area affect the heat transfer process significantly because of the increased conduction and convection. However the consideration of nanofluid also contributes significantly towards

* Corresponding author, e-mail: saleem366@yahoo.com

heat transfer enhancement as a consequence of its enhanced material properties. Being inspired by this fact we intend to investigate the heat transfer phenomena in the natural convection flow of a nanofluid near a vertical wavy wall.

The low thermal conductivity of commonly known pure fluids such as air or water is the main drawback against the heat transfer enhancement in the natural convection flows. A mixture of pure fluid and nanometer-sized material particle is termed as *nanofluid* [1]. These fluids are engineered colloidal suspensions of nanoparticles in the base fluid. The nanoparticles used in nanofluid are typically made of metals, oxides, carbides, or carbon nanotubes. The base fluids used are usually (but not limited to) water, ethylene, glycol, oil, *etc.* Because of their improved material properties nanofluids have many applications in industry such as coolants, lubricants, heat exchangers, micro-channel heat sinks, *etc.* Nanofluids have expressed unexpected properties which has increased their acceptance, particularly, in heat and mass transfer sciences. Masuda *et al.* [2] noted the enhancement of thermal conductivity in advance nuclear system by using nanofluid. Nanofluids have a distinctive characteristic which are quite different from those of traditional solid-liquid mixtures in which millimeter or micrometer-sized particles are involved. Such particles can clot equipment and can increase pressure drop due to settling effects. Moreover, being large in size they settle rapidly creating substantial additional pressure as pointed out by Khanafer *et al.* [3]. Enhanced thermal conductivity is not a single benefit of adding the nanoparticle but there are other factors such as nanoparticle size, volume fraction, particle agglomeration, Brownian motion, thermophoresis, particle shape, temperature, and nanoparticle-liquid interface.

Pohlhausen [4] was the first who first analyzed the steady free convection flow of a viscous incompressible fluid past a semi-infinite vertical plate by using integral method. Ostrach [5] presented the similarity solution of natural convection along vertical isothermal plate. Yao [6] analyzed natural convection heat transfer from vertical wavy surface using simple co-ordinate transformation to change the wavy surface into a flat surface. Moulic and Yao [7] discussed mixed convection heat transfer due to vertical wavy surface. Molla *et al.* [8] studied natural convection heat transfer from vertical wavy surface using uniform surface temperature with heat generation. Rees and Pop [9] studied the natural convection flow over a vertical wavy surface in porous media saturated with Newtonian fluid. Hossain and Rees [10] examined the heat and mass transfer in natural convection flow along a vertical wavy surface with constant wall temperature and concentration. Cheng [11] discussed the solution of heat and mass transfer in natural convection flow along a vertical wavy surface in porous medium. Saddiqa *et al.* [12] studied the radiation effects in natural convection flow along vertical wavy surface. Molla *et al.* [13] investigated natural convection flow along a vertical complex wavy surface with uniform heat flux by assuming thermal conductivity of the fluid as constant. Javed *et al.* [14] presented MHD effects of Cu-water nanofluid in a triangular cavity. Mustafa *et al.* [15] discussed MHD mixed convection stagnation point flow of a nanofluid over a vertical plate under the influence of viscous dissipation. Ghaffari *et al.* [16] investigated radiation effects on oblique stagnation point flow of a non-Newtonian nanofluid over stretching surface.

Being inspired from the mentioned studies the present work aims to investigate the impact of surface roughness and the nanofluid towards heat transfer enhancement in natural convection flow. The famous Tiwari and Das [17] model is being utilized to formulate the boundary-layer equations which are subsequently solved through implicit finite difference method. The results are discussed through graphs and tables and percent increase in rate of heat transfer is also calculated. It is observed that the nanofluid including gold nanoparticle is serves to be the best coolant in comparison to the other considered metals.

Mathematical formulation

Consider a vertical surface with transverse undulations following sinusoidal patterns. The surface texture of the vertical wavy surface is given by:

$$\bar{y}_w = \bar{S}(\bar{x}) = \bar{\alpha}\sin\left(\frac{\pi\bar{x}}{l}\right) \tag{1}$$

where $\bar{\alpha}$ is the fixed amplitude, and l – the fixed wave length. The origin of the co-ordinate system lies on the leading edge of the vertical surface as shown in fig. 1.

It is assumed that the surface temperature of the vertical wavy surface, T_w, is uniform and $T_w > T_\infty$, where T_∞ is the ambient temperature. The flow is assumed to be caused due to temperature difference between the wavy plate and the ambient fluid. Accordingly, the flow is steady and 2-D in nature. The study of convective transport in nanofluid requires a suitable model that can successfully capture the contribution of nanoparticle in flow and heat transfer phenomena. The aforementioned Tiwari and Das [17] model considers the improved material properties of the nanofluid. Practically, the nanoparticle contribute in convective phenomena in two ways: first by changing the material properties of the base fluid and secondly through their Brownian motion within the base fluid. The fluid properties are assumed to be described by the Tiwari and Das [17] model in this study. According to this model the 2-D boundary-layer mass, momentum, and energy conservation laws with the consideration of Boussinesq approximation are given by:

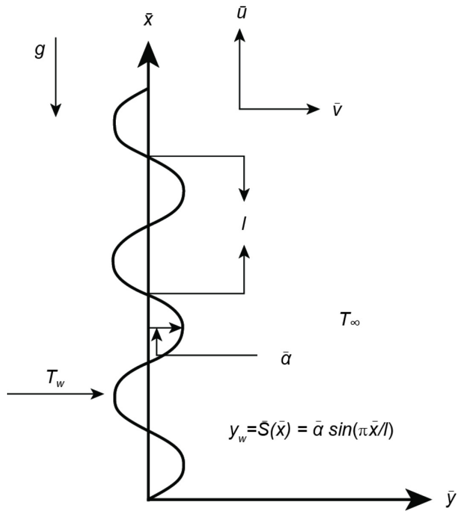

Figure 1. Physical model and co-ordinate system

$$\frac{\partial\bar{u}}{\partial\bar{x}} + \frac{\partial\bar{v}}{\partial\bar{y}} = 0 \tag{2}$$

$$\bar{u}\frac{\partial\bar{u}}{\partial\bar{x}} + \bar{v}\frac{\partial\bar{u}}{\partial\bar{y}} = -\frac{1}{\rho_{\mathrm{nf}}}\frac{\partial\bar{p}}{\partial\bar{x}} + \nu_{\mathrm{nf}}\nabla^2\bar{u} + \frac{1}{\rho_{\mathrm{nf}}}\mathrm{g}(\rho\beta)_{\mathrm{nf}}(T - T_\infty) \tag{3}$$

$$\bar{u}\frac{\partial\bar{v}}{\partial\bar{x}} + \bar{v}\frac{\partial\bar{v}}{\partial\bar{y}} = -\frac{1}{\rho_{\mathrm{nf}}}\frac{\partial\bar{p}}{\partial\bar{y}} + \nu_{\mathrm{nf}}\nabla^2\bar{v} \tag{4}$$

$$\bar{u}\frac{\partial T}{\partial\bar{x}} + \bar{v}\frac{\partial T}{\partial\bar{y}} = \alpha^*_{\mathrm{nf}}\nabla^2 T \tag{5}$$

where T is the temperature, $\bar{p}$ – the pressure, g – the gravitational acceleration, β_{nf} – the thermal expansion coefficient, ρ_{nf} – the density, α^*_{nf} – the thermal diffusivity of the nanofluid,

∇^2 – the Laplacian operator, $\overline{u}$ and $\overline{v}$ are the components of velocity along the $\overline{x}$ - and $\overline{y}$ -directions, respectively. The relations for μ_{nf}, ρ_{nf}, $(\rho\beta)_{\text{nf}}$, α^*_{nf}, and $(\rho c_p)_{\text{nf}}$ are given by:

$$\mu_{\text{nf}} = \frac{\mu_{\text{f}}}{(1-\phi)^{2.5}}, \quad (\rho c_p)_{\text{nf}} = (1-\phi)(\rho c_p)_{\text{f}} + \phi(\rho c_p)_p, \quad \rho_{\text{nf}} = (1-\phi)\rho_{\text{f}} + \phi\rho_p,$$
$$(\rho\beta)_{\text{nf}} = (1-\phi)(\rho\beta)_f + \phi(\rho\beta)_p, \quad \alpha^*_{\text{nf}} = \frac{\kappa_{\text{nf}}}{(\rho c_p)_{\text{nf}}}, \quad \frac{\kappa_{\text{nf}}}{\kappa_{\text{f}}} = \frac{(\kappa_p + 2\kappa_{\text{f}}) - 2\phi(\kappa_{\text{f}} - \kappa_p)}{(\kappa_p + 2\kappa_{\text{f}}) + \phi(\kappa_{\text{f}} - \kappa_p)} \tag{6}$$

in which ρ, (ρc_p), and κ are the density, heat capacity, and thermal conductivity, respectively. The thermal conductivity κ_{nf} of nanofluid was first used by Garnett [18] in 1904. The subscripts, f, p, and nf refer to the base fluid, nanoparticle, and the nanofluid, respectively, and ϕ – the solid volume fraction of nanoparticle.

According to the co-ordinate system along with the assumed flow conditions, the appropriate boundary conditions for the velocity components and temperature function are described:

$$\overline{y} = \overline{S}(\overline{x}) : \overline{u} = \overline{v} = 0, \quad T = T_w, \qquad \overline{y} \to \infty : \overline{u} = 0, \quad \overline{p} = p_\infty, \quad T = T_\infty \tag{7a}$$

Since the boundary-layer starts to develop at $x > 0$, therefore at the leading edge $x = 0$ the ambient flow conditions are assumed to be valid which are given by:

$$\overline{x} = 0 \;\; \overline{p} = p_\infty, \quad T = T_\infty, \quad \text{for all} \quad \overline{y} \neq 0 \tag{7b}$$

In this case the characteristic length is the wave length, l, and all the lengths are non--dimensionalized by l. Temperature difference $T_w - T_\infty$ is used to non-dimensionalize the temperature function. The surface undulations are assumed to be small enough such that $\overline{\alpha} \ll \overline{\delta}$ where $\overline{\delta}$ is the boundary-layer thickness. This assumption provides the reason for neglecting the pressure term $\partial\overline{p}/\partial\overline{x}$ in eq. (3). In this way the governing equations in dimensionless form under the boundary-layer assumptions read:

$$\frac{\sigma^2}{m_1} f''' + \frac{3}{4} ff'' - \frac{1}{2} f'^2 + \frac{m_4}{m_2}\theta = \xi\left(f'\frac{\partial f'}{\partial \xi} - f''\frac{\partial f}{\partial \xi} \right) \tag{8}$$

$$\frac{m\sigma^2}{m_3 \Pr}\theta'' + \frac{3}{4} f\theta' = \xi\left(f'\frac{\partial \theta}{\partial \xi} - \theta'\frac{\partial f}{\partial \xi} \right) \tag{9}$$

where the dimensionless variables are described:

$$\xi = x = \frac{\overline{x}}{l}, \quad y = \frac{\overline{y} - \overline{S}(\overline{x})}{l}\text{Gr}^{1/4}, \quad u = \frac{\rho_{\text{fl}}}{\mu_{\text{f}}}\text{Gr}^{-1/2}\,\overline{u}, \quad v = \frac{\rho_{\text{fl}}}{\mu_{\text{f}}}\text{Gr}^{-1/4}(\overline{v} - S_\xi \overline{u}),$$
$$S = \frac{\overline{S}(\overline{x})}{l}, \quad \theta(\xi, \eta) = \frac{T - T_\infty}{T_w - T_\infty}, \quad \psi(\xi, \eta) = \xi^{3/4} f(\xi, \eta), \quad \eta = \xi^{-1/4} y, \tag{10}$$
$$p = \frac{l^2}{\rho_{\text{f}}}\text{Gr}^{-1/4}\,\overline{p}, \quad u = \frac{\partial \psi}{\partial x}, \quad v = -\frac{\partial \psi}{\partial y}$$

where f is the dimensionless stream function, $\text{Gr} = g\beta_{\text{f}}(T_w - T_\infty)l^3/\nu_{\text{f}}^2$ the Grashof number, $\Pr = \nu_{\text{f}}/\alpha_{\text{f}}$ – the Prandtl number, the subscript ξ denotes derivative with respect to ξ and ' denotes differentiation with respect to η. The parameter $\sigma = (1 + S_\xi^2)^{1/2}$ denote the wavy contribution in the governing equations, where S_ξ denotes the partial derivative of S with respect to ξ. The material parameters m, m_1, m_2, m_3, and m_4 are given by:

$$m=\frac{\kappa_{\mathrm{nf}}}{\kappa_{\mathrm{f}}},\quad m_1=(1-\phi)^{2.5}\left(1-\phi+\phi\frac{\rho_p}{\rho_{\mathrm{f}}}\right),\quad m_2=1-\phi\phi\frac{\rho_p}{\rho_{\mathrm{f}}}$$
$$m_3=\left[1-\phi+\phi\frac{(\rho c_p)_p}{(\rho c_p)_f}\right],\quad m_4=\left[1-\phi+\phi\frac{(\rho\beta)_p}{(\rho\beta)_f}\right] \tag{11}$$

Following eq. (10), the boundary conditions in dimensionless form are described:

$$f(\xi,0)=0,\quad f'(\xi,0)=0,\quad \theta(\xi,0)=1,\quad f'(\xi,0)=0,\quad \theta(\xi,0)=0 \tag{12}$$

The parameters of physical interest in the current heat transport problem are the skin friction coefficient and the local Nusselt number which are defined:

$$C_{fx}=\frac{\tau_w}{\rho_{\mathrm{f}}U^2},\quad \mathrm{Nu}_x=\frac{\overline{x}q_w}{\kappa_{\mathrm{f}}(T_w-T_\infty)} \tag{13}$$

where $U = [(\mu_{\mathrm{f}})/(l\rho_{\mathrm{f}})]\mathrm{Gr}^{1/2}$ is the characteristic velocity, τ_w – the wall shear stress, and q_w – the wall heat flux which are given by:

$$\tau_w=\mu_{\mathrm{nf}}(\nabla\overline{u}\cdot\hat{n})_{y=0},\quad q_w=-\kappa_{\mathrm{nf}}(\nabla\overline{u}\cdot\hat{n})_{y=0} \tag{14}$$

where $\hat{n}=(-S_\xi/\sigma, 1/\sigma)$ is the unit normal to the wavy surface, and ∇ – the gradient operator. After using eqs. (10) and (14), the skin friction coefficient and local Nusselt number takes the form:

$$C_f=C_{fx}\left(\frac{\mathrm{Gr}}{x}\right)^{1/4}=\frac{\sigma}{(1-\phi)^{2.5}}f''(\xi,0),\qquad \mathrm{Nu}=\mathrm{Nu}_x(\mathrm{Gr}\,x^3)^{-1/4}=-\sigma\frac{\kappa_{\mathrm{nf}}}{\kappa_{\mathrm{f}}}\theta'(\xi,0) \tag{15}$$

The dimensionless average skin friction and average Nusselt number are defined:

$$C_{f\mathrm{avg}}=\frac{1}{\mathbb{S}}\int_0^\xi\frac{x^{1/4}\sigma^2}{(1-\phi)^{2.5}}f''(\xi,0)\mathrm{d}\xi,\qquad \mathrm{Nu}_{\mathrm{avg}}=-\frac{1}{\mathbb{S}}\int_0^\xi dx^{3/4}\sigma^2\theta'(\xi,0)\mathrm{d}\xi \tag{16}$$

where $\mathbb{S}=\int_0^\xi\omega\mathrm{d}\xi$ is the surface area of the wavy sheet over an unit dimension. The average skin friction and average Nusselt number in eq. (16) have been calculated numerically.

Result and discussion

The governing non-similar eqs. (8) and (9) subject to boundary conditions (12) are solved numerically using an implicit finite difference scheme known as Keller-Box method [19-21]. In order to validate the present solution scheme, the already existing results by Alim *et al.* [22], Hossain *et al.* [23], and Kabir *et al.* [24] have been reproduced. A comparison between the present results and already existing data is given in tab. 1 where the results are in excellent agreement. This authenticates our present solution scheme and allows us to utilize it in solving the current equations.

The effects of nanoparticle volume fraction and wavy amplitude on the transient velocity and temperature profiles of the Cu-water nanofluid are plotted in figs. 2 and 3 for different values of α and ϕ. From fig. 2 it is observed that the velocity increases at crest and trough locations on the wavy surface but decreases at node. This fact is due to the increase in

Table 1. Comparison of present results with existing data at α = 0

Pr	$f''(0,0)$				$-\theta'(0,0)$			
	Present	Hossain *et al.* [23]	Alim *et al.* [22]	Kabir *et al.* [24]	Present	Hossain *et al.* [23]	Alim *et al.* [22]	Kabir *et al.* [24]
1	0.9082	0.908	0.90814	0.90813	0.4010	0.401	0.40101	0.40102
10	0.5928	0.591	0.59269	0.59270	0.8268	0.825	0.82663	0.82662
25	0.4876	0.485	0.48733	0.48732	1.0690	1.066	1.06847	1.06848
50	0.4176	0.485	0.41727	0.41728	1.2896	1.066	1.28879	1.28878
100	0.3559	0.352	0.35559	0.35558	1.5495	1.542	1.54827	1.54828

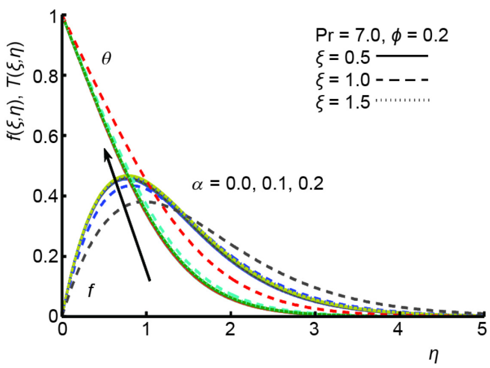

Figure 2. The effect of α on velocity and temperature profile

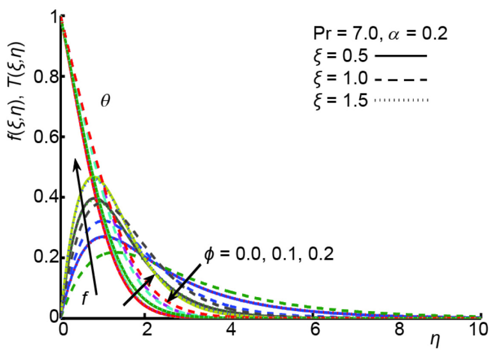

Figure 3. The effect of ϕ on velocity and temperature profile

values of α which highlights the role of surface undulation towards enhanced convection. Figure 3 displays the influence of various values of the nanoparticle volume fractions ϕ on velocity profile. It can be seen from fig. 3 that the velocity profile decreases at crest, node and trough locations on the wavy surface on increasing ϕ but velocity is minimum at node as compared to crest and trough. The temperature profiles under the influence of same values of α and ϕ ($\phi = \alpha$ = 0.0, 0.1, 0,2) are also plotted in figs. 2 and 3, respectively. The effect of α on temperature profile is shown in fig. 2. It is seen that variation in α does not bring significant change in the temperature profile at crest and trough positions but increases at node. Figure 3 shows the influence of various values of the nanoparticle volume fractions ϕ on temperature distribution. It is noted that the thermal boundary-layer thickness increases by increasing the values of ϕ. Since the cooper has high thermal conductivity therefore the maximum increase in thickness is observed for Cu-water nanofluid. Figures 4 and 5 depict the variations of the local skin friction coefficient and the local Nusselt number with increasing values of wavy amplitude α for Cu-water nanoparticle. An increase in α results in increasing the wavy amplitude of the curves which further grows downstream keeping the wavelengths constant in both graphs. The variation of skin friction and Nusselt number with ϕ is shown in figs. 6 and 7, respectively. Evidently the volume fraction parameter does not effect the skin friction significantly as compared to the Nusselt number. This fact highlights the direct impact of nanoparticle concentration on the heat transfer rate.

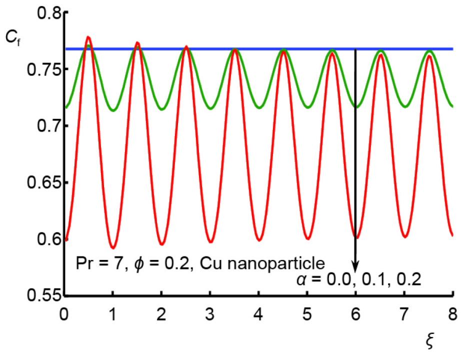

Figure 4. Skin friction graph for different values of α

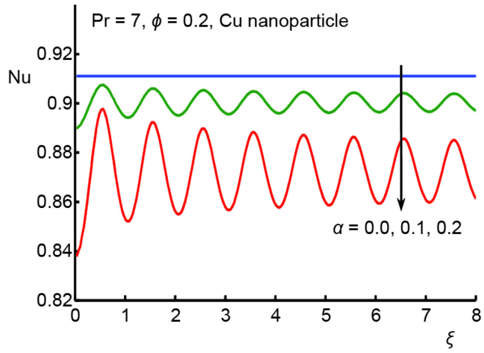

Figure 5. Nusselt number plotted against ξ for different values of α

The current analysis has been carried out for five different types of nanoparticles, namely, Ag, Cu, Al_2O_3, Fe_3O_4, and SiO_2. Table 2 shows the thermophysical properties of water and the five elements Ag, Cu, Al_2O_3, Fe_3O_4, and SiO_2. Here we investigate the effect of different nanoparticle on skin friction and heat transfer on a vertical wavy surface. To compare the Skin friction and heat transfer for different nanoparticle, where base liquid is considered to be water. It is worth mentioning here that this study reduces the governing eqs. (8) and (9) to those of a pure or regular fluid when $\phi = 0$. Skin friction and Nusselt number are plotted against the solid volume fraction ϕ and wavy amplitude α for different type of nanoparticles (Ag, Cu, Al_2O_3, Fe_3O_4, and SiO_2) in figs. 8-11. Figures 8 and 9 illustrate the variations of the local skin friction coefficient and the local Nusselt number with nanoparticle volume fraction parameter ϕ. These figures show that these quantities increase almost linearly with ϕ and maximum increase in skin friction is observed for Ag and in Nusselt number for Cu. This shows that the presence of the nanoparticles in the base fluid increases the effective thermal conductivity of the fluid quite appreciably and consequently enhances the heat transfer characteristics as seen in these figures. Similarly the variation in local skin friction and Nusselt number against wavy amplitude is shown in figs. 10 and 11 for different nanoparticles. Clearly the variation due to these parameters is almost linear but the nature of nanoparticle does matter. Maximum increase in skin friction is observed for Ag and in Nusselt number for Cu. It is worth mentioning that according to eq. (15) the Nusselt number is a product of the temperature gradient and the thermal conductivity ratio (conductivity of the nanofluid to the conduc-

Table 2. Thermophysical properties of base fluid and nanoparticle

Properties	C_p [Jkg^{-1}K^{-1}]	ρ [kgm^{-3}]	κ [Wm^{-1}K^{-1}]	$\beta\cdot10^{-5}$ [K^{-1}]
Fluid (water)	4179	997.1	0.613	21.0
Au	128	19320	318	0.01416
Ag	235	10500	429	1.89
Cu	383.1	8954	386	1.67
Al_2O_3	765	3970	40	0.85
Fe_3O_4	670	5180	9.7	0.5
SiO_2	703	2200	1.2	0.056

tivity of the base fluid). Increasing ϕ leads to an increase in the thermal conductivity ratio which in turn increases the Nusselt number. Isotherms are plotted for same values of α and ϕ ($\alpha = \phi =$ $= 0.0, 0.1, 0{,}2$) in figs. 12 and 13. The wavy pattern can easily be seen in the isotherm graphs.

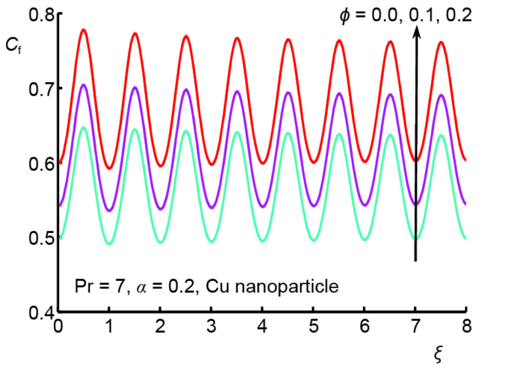

Figure 6. Skin friction profile for different values of ϕ

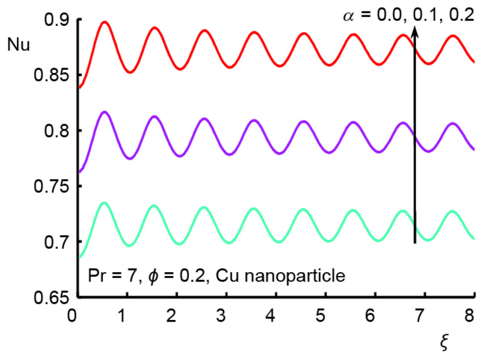

Figure 7. Nusselt number graph for different values of ϕ

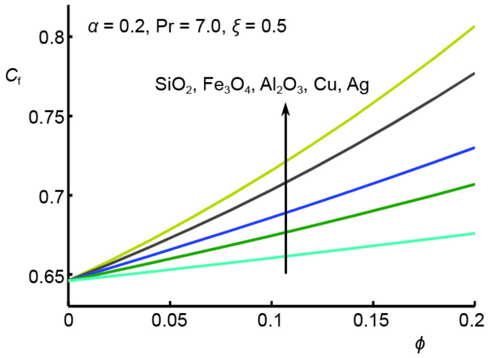

Figure 8. Effect of ϕ on skin friction for different nanoparticles

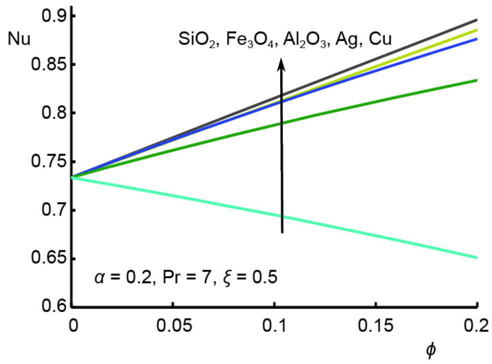

Figure 9. The effect of ϕ on Nusselt number for different nanoparticles

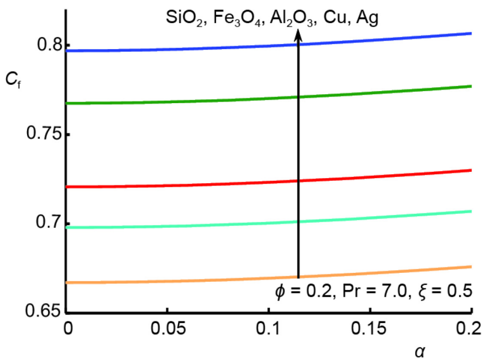

Figure 10. The effect of α on skin friction for different nanoparticle

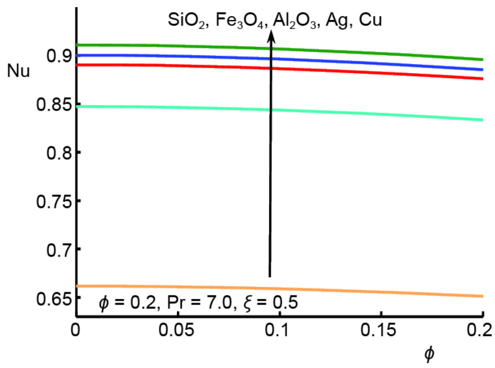

Figure 11. The effect of α on Nusselt number for different nanoparticles

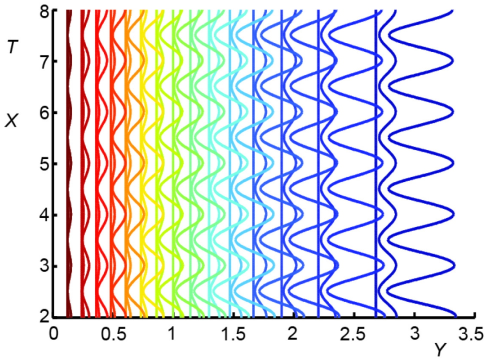

Figure 12. Isotherms plotted at different α
(*for color image see journal web site*)

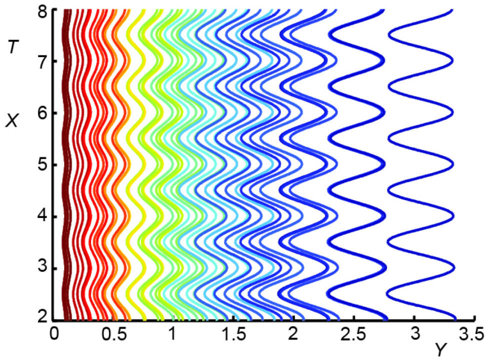

Figure 13. Effect of different ϕ on isotherms
(*for color image see journal web site*)

Numerical values of skin friction and rate of heat transfer for different values of α and ϕ when Pr = 7.0 for Cu on the vertical wavy surface at x = 0.5, x = 1.0, and x = 1.5 are presented in tab. 3. It is observed that the both Nusselt number and skin friction increase with the increase of ϕ and the skin friction increases and Nusselt number decreases with increase of α. Table 4 shows percent change in skin friction and Nusselt number for Cu nanoparticle for different values of α and ϕ when Pr = 7.0 in comparison to wavy and flat vertical plate at three different locations; crest, node, and trough on the vertical wavy surface. It is observed that at crest skin friction increases and Nusselt number decreases by increasing the wavy amplitude at fixed concentration of nanoparticle. Similarly for a fixed value of α both skin friction and Nusselt number increase by increasing the nanoparticle concentration. The similar

Table 3. Variation in skin friction and Nusselt number for different values of α and ϕ when Pr = 7.0 for Cu

ξ	ϕ	α	C_f	Nu
0.5 (Crest)	0.2	0.0	0.7675	0.9111
		0.1	0.7702	0.9070
	0.0	0.2	0.6460	0.7337
	0.1		0.7034	0.8151
	0.2		0.7771	0.8959
1.0 (Node)		0.0	0.6567	0.8224
		0.1	0.7134	0.8947
	0.0	0.2	0.4914	0.6971
	0.1		0.5358	0.7757
	0.2		0.5927	0.8536
1.5 (Trough)	0.2	0	0.6567	0.8224
		0.1	0.7688	0.9055
	0	0.2	0.6437	0.7312
	0.1		0.6997	0.8111
	0.2		0.7721	0.8906

behavior is followed by the skin friction and Nusselt number at the trough location but at the node both skin friction and Nusselt number increase with the increase of wavy amplitude and concentration of nanoparticle. The nature of nanoparticle has fundamental role in enhancing the convective heat transfer phenomena. Nanoparticle of five different materials (Ag, Cu, Al_2O_3, Fe_3O_4, and SiO_2) including two metals and three oxides have been considered in tab. 5 towards the calculations of percent increase in the magnitude of skin friction and the Nusselt number. It is observed that maximum increase in metals of about 24.9% in skin friction is obtained for Ag with 20% concentration in the base fluid and minimum increase in metals of about 20.3% in the value of skin friction is obtained for Cu with 20% concentration when the present results are compared with the value $f''(0.5, 0) = 0.6460$ at $\alpha = 0.2$, and $\phi = 0.0$. Similarly for oxides, maximum increase of about 13% in skin friction is obtained for Al_2O_3 with 20% concentration in the base fluid and minimum increase of about 4.7% in the value of skin friction is obtained for SiO_2 with same concentration. On the other hand for metals, maximum gain in metal of about 22.1% in Nusselt number is obtained for Cu and minimum of 20.7% for Ag with 20% concentration in the base fluid when the present results are compared with Nu = 0.7337 at $\alpha = 0.2$ and $\phi = 0.0$. Similarly, for oxides, maximum increase of about 19.4% in Nusselt number is obtained for Al_2O_3 with 20% concentration in the base fluid and minimum decrease of about 11.2% in the value of Nusselt number is obtained for SiO_2 with same concentration. The percent increase in skin friction and Nusselt number is also calculated in comparison to $f'' = 0.6375$ and Nu = 0.7455 at $\alpha = 0.0$ and $\phi = 0.0$. For metals, maximum of 26.5% and 20.2% increase in skin friction and Nusselt number is obtained and a minimum of

Table 4. Percent increase in skin friction and Nusselt number for Cu in comparison to pure fluid ($\phi = 0$) with wavy ($\alpha \neq 0$) and flat plate ($\alpha = 0$) case when Pr = 7.0

ξ	α	ϕ	% increase in C_f		% increase in Nusselt number	
			Verses wavy plate at $\phi = 0.0$	Verses flat plate at $\phi = 0.0$	Verses wavy plate at $\phi = 0.0$	Verses flat plate at $\phi = 0.0$
0.5 (Crest)	0.0	0.2	–	20.4	–	22.2
	0.1		20.4	20.8	22.2	21.7
	0.2	0.0	0.0	2.7	0.0	–1.6
		0.1	8.9	10.3	11.1	9.3
			20.3	21.9	22.1	20.2
1.0 (Node)	0.0	0.2	–	20.4	–	22.2
	0.1		20.5	11.9	22.2	20.0
	0.2	0.0	0.0	–22.9	0.0	–6.5
		0.1	9.0	–15.9	11.3	4.1
			20.6	–7.0	22.5	14.5
1.5 (Trough)	0.0	0.2	–	20.4	–	22.2
	0.1		20.3	20.6	22.1	21.5
	0.2	0.0	0.0	–0.4	0.0	–1.9
		0.1	8.7	9.7	10.9	8.8
		0.2	19.9	21.1	21.8	19.5

21.9% and 18.8% increase in skin friction and Nusselt number is obtained, respectively. Similarly for oxides, maximum of 14.5% and 17.5% increase in skin friction and Nusselt number is obtained and a minimum of 6.1% increase in skin friction and 12.6% decrease in Nusselt number is obtained, respectively. Through tab. 5 it is easy to identify the role of surface roughness and of nanofluid towards heat transfer enhancement.

Table 5. Percent change in skin friction and Nusselt number for different nanoparticle when Pr = 7.0, α = 0.2, ϕ = 0.2

ξ	Nanoparticle material	% increase in $-C_f$		% increase in Nusselt number	
		Verses $f'' = 0.6375$ at $\alpha = \phi = 0.0$	Verses $f''(0.5,0) = 0.6460$ at $\alpha = 0.2, \phi = 0.0$	Verses Nu = 0.7455 at $\alpha = \phi = 0.0$	Verses Nu = 0.7337 at $\alpha = 0.2, \phi = 0.0$
0.5	Au	4.2	2.8	8.4	10.1
	Ag	26.5	24.9	18.8	20.7
	Cu	21.9	20.3	20.2	22.1
	Fe_3O_4	10.9	9.4	11.8	13.6
	Al_2O_3	14.5	13.0	17.5	19.4
	SiO_2	6.1	4.7	-12.6	-11.2

Conclusions

In the present study, we have numerically investigated the natural convection heat transfer of nanofluid along five different types of nanoparticles, Ag, Cu, Al_2O_3, Fe_3O_4, and SiO_2 with a valid range of particle concentration (0-20%) by taking water as base fluid. An excellent agreement between the present results and already published data proves the validity of present results. Our analysis reveals that:

- The skin friction increases and Nusselt number decreases by increasing the values of wavy amplitude α.
- An increase in concentration of nanoparticles in the base fluid produces an increase in the skin friction coefficient and the local Nusselt number.
- Maximum increase in skin friction is about 24.9% for Ag and in Nusselt number is about 22.1% for Cu with 20% concentration.]]
- Minimum increase in skin friction is about 4.7% and in Nusselt number is –11.2% for SiO_2 with 20% concentration.

Acknowledgment

The authors are grateful to the anonymous reviewer's valuable comments that improved the manuscript.

Nomenclature

c_p – specific heat, [$Jkg^{-1}K^{-1}$]
f – dimensionless stream function, [–]
g – acceleration of gravity, [ms^{-2}]
l – characteristic length of the wavy plate, [m]
Pr – Prandtl number, [–]
p – dimensionless pressure, [–]
$\bar{p}$ – dimensional pressure, [$kgms^{-2}$]
S – dimensional wavy surface parameter, [–]
T – local temperature, [K]
(u, v) – velocity component in x- y-direction, [–]
$(\bar{u}, \bar{v})$ – velocity component in $\bar{x}$-$\bar{y}$-direction, [ms^{-1}]
(x, y) – dimensionless co-ordinates, [–]

$(\bar{x}, \bar{y})$ – dimensional co-ordinates, [m]

Greek symbols

α – dimensionless amplitude of the wavy surface, [–]
$\bar{\alpha}$ – dimensional amplitude of the wavy surface, [m]
ξ, η – new computational independent variables, [–]
α^* – thermal diffusivity, [m^{2}s^{-1}]
β – coefficient of thermal expansion, [K^{-1}]
θ – dimensionless temperature, [–]
κ – thermal conductivity, [Wm^{-1}K^{-1}]
μ – dynamic viscosity, [kgms^{-1}s^{-1}]
ρ – local density, [kgms^{-3}]
ν – kinematic viscosity, [m^{2}s^{-1}]
σ – electrical conductivity, [Ωm]
ϕ – solid volume friction
ψ – dimensionless stream function, [kgm^{-1}s^{-1}]

Subscripts

f – base fluid
nf – nanofluid
p – nanoparticle
w – condition at the surface
∞ – condition far away from surface

References

[1] Choi, S. U. S., Enhancing Thermal Conductivity of Fluids with Nanoparticles, *ASME, FED*, *132* (1995), 66, pp. 99-105
[2] Masuda, H., *et al*., Alteration of Thermal Conductivity and Viscosity of Liquid by Dispersing Ultra-Fine Particles, *Netsu Bussei, 7* (1993), 4, pp. 227-233
[3] Khanafer, K., *et al*., Buoyancy-Driven Heat Transfer Enhancement in a Two-Dimensional Enclosure Utilizing Nanofluids. *Int. J. Heat Mass Transfer, 46* (2003), 19, pp. 3639-3653
[4] Pohlhausen, E., Der Wärmeaustausch zwischen festen Körpern und Flüsigkeiten mit Kleiner Reibung und Kleiner Wärmeleitung, *Zeitschrift für Angewandte Mathematik und Mechanik*, *1* (1921), 2, pp. 115-121
[5] Ostrach, S., An Analysis of Laminar Free Convective Flow and Heat Transfer about a Flat Plate Parallel to Direction of the Generating Body Force, Report No. 1111, NASA, Vashington, USA, 1953
[6] Yao, L. S., Natural Convection along a Vertical Wavy Surface, *ASME J. Heat Transf., 105* (1983), 3, pp. 465-468
[7] Moulic, S. G., Yao, L. S., Natural Convection along a Wavy Surface with Uniform Heat Flux, *ASME J. Heat Transf., 111* (1989), Nov., pp. 1106-1108
[8] Molla, M. M., *et al*., Natural Convection Flow along a Vertical Wavy Surface with Heat Generation/Absorption, *Int. J. Therm. Sci.*, *43* (2004), 2, pp. 157-163
[9] Rees, D. A. S., Pop, I., A Note on a Free Convection along a Vertical Wavy Surface in a Porous Medium, *ASME J. of Heat Transf.*, *116* (1994), 2, pp. 505-508
[10] Hossain, M. A., Rees, D. A. S., Combined Heat and Mass Transfer in Natural Convection Flow from a Vertical Wavy Surface, *Acta Mechanica, 136* (1999), 3-4, pp. 133-141
[11] Cheng, C. Y, Natural Convection Heat and Mass Transfer near a Vertical Wavy Surface with Constant Wall Temperature and Concentration in a Porous Medium, *Int. Commun, Heat and Mass Transf., 27* (2000), 8, pp. 1143-1154
[12] Siddiqa, S., *et al*., Natural Convection Flow with Surface Radiation along a Vertical Wavy Surface. Num, *Heat Transf., 64* (2013), 5, pp. 400-415
[13] Molla, M. M., *et al*., Natural Convection Flow along a Vertical Wavy Surface with Uniform Surface Temperature in Presence of Heat Generation/Absorption, *Int. J. Therm. Sci., 43* (2004), 2, pp. 157-163
[14] Javed, T., *et al*., Effects of Uniform Magnetic Field on the Natural Convection of Cu-Water Nanofluid in a Triangular Cavity, *Int. J. Num. Meh. Heat Fliud Flow*, *27* (2016), 2, pp. 334-357
[15] Mustafa, I., *et al*., Magnetohydrodynamic (MHD) Mixed Convection Stagnation Point Flow of a Nanofluid over a Vertical Plate with Viscous Dissipation, *Canad. J. Phy.*, *93* (2015), 11, pp. 1365-1374
[16] Ghaffari, A., *et al*., Oblique Stagnation Point Flow of a Non-Newtonian Nanofluid over Stretching Surface with Radiation, A numerical study, *Thermal Science*, *21* (2015), 5, pp. 2139-2153
[17] Tiwari, R. K., Das, M. K., Heat Transfer Augmentation in a Two-Sided Lid-Driven Differentially Heated Square Cavity Utilizing Nanofluids, *Int. J. Heat Mass Transf., 50* (2007), 9-10, pp. 2002-2018
[18] Maxwell G. J. C., Colours in Metal Glasses and in Metallic Films, *Philos. Trans. R. Soc. Lond. A*, *203* (1904), pp. 385-42
[19] Cebeci, T., *et al*., *Physical and Computational Aspects of Convective Heat Transfer*, Springer, New York, USA, 1988

[20] Cebeci, T., *et al*., *Modeling and Computing of Boundary-Layer Flows Laminar, Turbulent and Transitional Boundary Layers in Incompressible and Compressible Flows*, Springer, New York, USA, 2005
[21] Na, T. Y., *Computational Methods in Engineering Boundary Value Problems*, Academic Press, New York, USA, 1979
[22] Alim, M. A., *et al*., Heat Generation Effects on Magnetohydrodynamic (MHD) Natural Convection Flow along a Vertical Wavy Surface with Variable Thermal Conductivity, *A. J. of Comput. Math., 2* (2012), 1, pp. 42-50
[23] Hossain, M. A, *et al*., Natural Convection of Fluid with Temperature Dependent Viscosity from Heated Vertical Wavy Surface, *ZAMP*, *53* (2002), 1, pp. 48-52
[24] Kabir, K. H., *et al*., Effect of Viscous Dissipation on MHD Natural Convection Flow along a Uniformly Heated Vertical Wavy Surface, *J. Theo. and App. Phy., 7* (2013), 31, pp. 1-8
[25] Bachok, N., *et al*., Flow and Heat Transfer Characteristics on a Moving Plate in a Nanofluid, *Int. J. Heat Mass Transfer, 55* (2012), 4, pp. 642-648

Paper submitted: October 8, 2015
Paper revised: April 8, 2016
Paper accepted: May 17, 2016